

## Improved Determination of Structural Changes of 2-Pyridone-(H<sub>2</sub>O)<sub>1</sub> upon Electronic Excitation

Robert Brause, Michael Schmitt,\* and Karl Kleinermanns\*

Heinrich-Heine-Universität, Institut für Physikalische Chemie I, D-40225 Düsseldorf, Germany

Received: November 15, 2006; In Final Form: February 27, 2007

The change of the 2-pyridone–water cluster (2PYH<sub>2</sub>O) structure upon electronic excitation is determined by a Franck–Condon analysis of the intensities in the fluorescence emission spectra obtained via excitation of three different vibronic bands as well as a structural fit based on the rotational constants of eight isotopomers that have been reported by Held and Pratt (*J. Am. Chem. Soc.*, **1993**, *115*, 9708]. A total of 93 emission band intensities were fit, together with the changes of rotational constants of 8 isotopomers. The geometry change upon electronic excitation to the  $\pi\pi^*$  state can be described by a strong and unsymmetrical elongation of the hydrogen bonds, a contraction of the OH bond involved in the cyclic cluster arrangement, and an unsymmetrical ring deformation. The resulting geometry changes are interpreted on the basis of ab initio calculations.

### 1. Introduction

The tautomeric equilibrium between 2-pyridone (2PY) and 2-hydroxy-pyridine (2HP)<sup>1–4</sup> and their water clusters<sup>5–9</sup> has found widespread interest as model system for tautomerization-induced mutagenic effects in the RNA nucleobase uracil,<sup>10</sup> which has the same hydrogen binding motif as 2PY. To properly bind to the complementary adenine nucleobase in its most stable amino form, according to the Watson–Crick model of RNA, uracil must exist in its diketo tautomeric form. The formation of rare tautomeric forms of uracil upon radiation with ultraviolet light is supposed to be one of the reasons for base mispairing.<sup>11</sup> Therefore, the study of geometry changes in electronically excited states of base analogues and their water complexes might give new insight into the mechanisms of formation of tautomers, which are minority species in the electronic ground state.

The electronic ground state of 2PY and 2HP has been investigated by Hatherley et al. and Tanjaroon et al. using microwave spectroscopy.<sup>2,3</sup> Both groups concluded planar structures for both tautomers in their electronic ground state. Nowak et al. measured matrix isolation infrared spectra of the tautomers 2PY and 2HP and assigned the ground-state vibrations of the planar tautomers.<sup>12</sup>

Maris et al. measured the rotational spectrum of the 2PY-(H<sub>2</sub>O)<sub>1</sub> complex.<sup>6</sup> Because of the smaller dipole moment, they were not able to obtain the spectra of the 2HP(H<sub>2</sub>O)<sub>1</sub> complex. A small inertial defect indicated that the cluster is slightly nonplanar.

Florio et al. reported fluorescence depletion infrared (FDIR) spectra of 2PY(H<sub>2</sub>O)<sub>1,2</sub> complexes in the NH/OH region and assigned the bands by means of density functional theory (DFT) calculations.<sup>5</sup> FDIR spectra of 2PY(H<sub>2</sub>O)<sub>1,2</sub> complexes in the NH/OH region for the electronic ground state as well as for the electronically excited state were reported by Matsuda et al.<sup>7,8</sup> They found a strong blue-shift upon electronic excitation for the bonded OH stretch vibration and a small redshift for the bonded NH stretch vibration.

From resonant two-photon ionization (R2PI), laser-induced fluorescence (LIF), and single vibronic level fluorescence (SVLF) spectra of 2PY, 2HP, and their water cluster, Nimlos et al. concluded that peaks A and B in the excitation spectrum of 2PY belong to two different nonplanar conformers in the electronic ground state.<sup>13</sup>

For the electronically excited state, the group of Pratt contributed the structures of the monomer,<sup>1</sup> the water cluster,<sup>14</sup> the homo-dimer,<sup>15,16</sup> and the 2PY••2HP hetero-dimer.<sup>17</sup> The rotationally resolved LIF spectra of the two peaks A and B of 2PY were analyzed by Held et al.<sup>1</sup> On the basis of the rotational constants, they concluded that both A and B share the same ground-state zero-point vibrational level and therefore result from different conformers in the S<sub>1</sub> state. A recent publication of Leutwyler's group discusses the possibility that band B is due to an out-of-plane vibration in the excited state, which connects two equivalent minima in a symmetrical double-minimum potential.<sup>18</sup>

The water complexes 2PY(H<sub>2</sub>O)<sub>1,2</sub> were characterized using rotationally resolved LIF by Held and Pratt.<sup>14</sup> For the monosolvated complex, they obtained and assigned the spectra of nine different isotopomers. Although the structure of the water moiety remains unchanged, they found large structural changes of the 2PY monomer geometry upon cluster formation.

Barone and Adamo calculated the solvent-assisted tautomerization between 2PY and 2HP using DFT.<sup>19</sup> Li et al. performed ab initio calculations at the MP2, CASSCF, and MR-CI level of theory to predict pathways of the tautomerization reaction from 2PY to 2HP.<sup>20</sup> They could show that the reaction barrier in the excited state is lowered by association of one and two water molecules.

Compared to the large number of structure determinations of molecules in their electronic ground states, much less is known about geometries in electronically excited states because standard methods like X-ray diffraction or microwave spectroscopy cannot be applied to electronically excited states. A methodical exception is rotationally resolved LIF spectroscopy, which yields the inertial parameters of the molecules under investigation for the ground state *and* the electronically excited state. However, the number of structural parameters ( $3N - 6$ )

\* Corresponding authors. Phone: +49 211 81 12100. Fax: +49 211 81 15195. E-mail: mschmitt@uni-duesseldorf.de; kleinermanns@uni-duesseldorf.de.

exceeds the number of rotational constants (three for nonplanar molecules) by far. Kraitchman<sup>21</sup> and Costain<sup>22</sup> showed how a complete structure determination can be performed using the inertial parameters of different isotopically substituted derivatives of the parent molecule. Owing to the large experimental effort, a sufficient number of different isotopomers for a complete, or nearly complete, structure determination in both electronic states was used in only a few studies.<sup>23</sup> A complementary approach to excited-state structures is facilitated by the Franck–Condon (FC) principle. According to the FC principle, the relative intensity of a vibronic band depends on the overlap integral of the vibrational wave functions of both electronic states. The changes of the rotational constants upon excitation of different isotopomers can be used simultaneously in the fit of the structural changes upon electronic excitation without referring to the ground-state structure. This fit is based on a nonlinear geometry optimization using a local Levenberg–Marquart variant or a global optimizer based on genetic algorithms.<sup>23,24</sup>

In the following, we will show how a fit to the rotational constants from several isotopomers of the 2PY(H<sub>2</sub>O) cluster and the intensities from fluorescence emission spectra, excited through different vibronic bands, can be used to improve the information on the geometry changes upon electronic excitation of this cluster.

## 2. Experimental and Computational Details

**Experiment.** The experimental setup for the dispersed fluorescence (DF) spectroscopy is described in detail in refs 25 and 26. In brief, 2PY was evaporated at 390 K and co-expanded through a pulsed nozzle with a 500  $\mu\text{m}$  orifice (General Valve) into the vacuum chamber using Helium co-expanded with water vapor as the carrier gas. To avoid the formation of larger water clusters, the water was kept at temperatures below 268 K. The output of a Nd:YAG (Spectra Physics, Quanta Ray Indi) pumped dye laser (Lambda-Physik, FL3002) was frequency doubled and crossed perpendicularly with the molecular beam. The fluorescence light was collected perpendicular to the laser, and the molecular beam and was imaged on the entrance slit of a 1 m monochromator (Jobin Yvon, 2400 grooves/mm blazed at 400 nm for first order). The dispersed fluorescence was recorded by an intensified CCD camera (Flamestar II, LaVision). This allows us to image simultaneously a DF spectrum of about 500  $\text{cm}^{-1}$ . Accordingly, the relative intensities in our DF spectra do not vary with laser power. Only the intensity of the excited band is perturbed by scattered light. Thus, we normalize relative intensities with respect to the strongest band in the spectrum other than the resonance fluorescence band. The intensity uncertainty of the whole detection system was checked by shifting a particular fluorescence line over the CCD chip by changing the grating position. The observed intensity error was 10% at maximum.

**Ab Initio Calculations.** Ab initio calculations at the Møller–Plesset second-order (MP2) perturbation level of theory and DFT calculations have been carried out using the Gaussian 03 program package.<sup>27</sup> The self-consistent field (SCF) convergence criterion used throughout the calculations was an energy change below  $10^{-8}$  hartree and a convergence criterion for the gradient optimization of the molecular geometry of  $\partial E/\partial r < 1.5 \times 10^{-5}$  Hartree/Bohr and of  $\partial E/\partial \varphi < 1.5 \times 10^{-5}$  hartree/degrees, respectively. Dunning’s correlation-consistent polarized valence triple- $\zeta$  basis set (cc-pVTZ) was used for the MP2 and B3LYP calculations.<sup>28</sup> Complete active space self-consistent field (CASSCF) calculations were performed with the MOLCAS

**TABLE 1: S<sub>0</sub> State Geometry Parameters of 2PYH<sub>2</sub>O, Calculated at the B3LYP/cc-pVTZ, MP2/cc-pVTZ, and CASSCF(8,7)/cc-pVDZ Levels of Theory<sup>a</sup>**

S <sub>0</sub>	B3LYP	MP2	CASSCF	expt <sup>14</sup>
A''/MHz	3994	3989	3944	3997
B''/MHz	1411	1432	1343	1394
C''/MHz	1045	1056	1005	1035
$\Delta I/u \cdot \text{Å}^2$	-1.09	-1.03	-1.58	-0.60
N1–C2	139.6	139.0	137.3	
C2–C3	144.0	143.8	146.5	
C3–C4	136.2	136.9	135.8	
C4–C5	141.8	141.5	144.5	
C5–C6	136.0	136.5	135.4	
C6–N1	135.5	135.6	137.4	
C2–O7	123.7	124.2	121.5	
N1–H1	102.3	102.4	100.5	
O8–H7	98.2	98.1	95.4	
O8–H8	96.1	96.0	94.7	
O7–H7	182.8	178.8	207.3	197.0
O8–H	193.5	188.2	208.7	196.0
N1–O8	283.5	278.5	297.9	286.0
O7–O8	273.7	271.0	290.6	277.0
C3–H	108.0	107.9	108.0	
C4–H	108.3	108.2	108.2	
C5–H	107.8	107.8	107.9	
C6–H	108.0	108.0	107.9	

<sup>a</sup> The atomic numbering refers to Figure 1. All bond lengths are given in pm.

program package (Version 6.0)<sup>29</sup> for the ground as well as for the first excited state of 2PYH<sub>2</sub>O. The complete  $\pi$  space (8,7) of the pyridone moiety including the lone pair of the N1 atom with correct  $\pi$  symmetry was utilized as active space with Dunning’s correlation-consistent polarized valence double- $\zeta$  basis set (cc-pVDZ).<sup>28</sup> One lone pair, localized at the oxygen atom of the water moiety with near  $\pi$  symmetry, was discarded because of its low energy. The calculations were performed on a SGI Origin2000 (MOLCAS), a Sun Fire 15K (Gaussian 03), and a Sun Opteron Cluster (TURBOMOLE).

**Structure Fits.** The change of a molecular geometry upon electronic excitation can be determined from the intensities of absorption or emission bands using the FC principle. According to the FC principle, the relative intensity of a vibronic band depends on the overlap integral of the vibrational wave functions of both electronic states, which is determined by the relative shift of the two potential energy curves connected by the vibronic transition along the normal coordinates of both states. The program FCFit<sup>30</sup> determines the structural changes upon electronic excitation from the experimentally determined intensity pattern as has been shown in a previous publication. The structure of molecules or molecular clusters can be determined from the rotational constants of several isotopomers. The program *pKrFit*, which has been described previously,<sup>23,24</sup> uses a gradient-based  $\chi^2$  minimizer as well as a genetic algorithm (GA) based global optimizer in order to determine the ground- and excited-state structures.

## 3. Results

**Ab Initio Calculations.** The ground-state structure of 2PYH<sub>2</sub>O was optimized at the MP2/cc-pVTZ, B3LYP/cc-pVTZ, and CASSCF(8,7)/cc-pVDZ levels of theory. The S<sub>1</sub> state geometry was optimized at the CASSCF(8,7)/cc-pVDZ level of theory. For both ground and excited state, the harmonic vibrational frequencies were calculated using the analytical second derivatives of the potential energy.

The resulting geometry parameters are presented in Table 1. The atomic numbering in Table 1 refers to Figure 1.

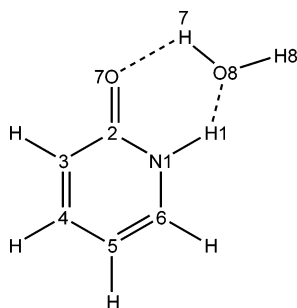


**Figure 1.** Atomic numbering of the 2-pyridone–water cluster.

Table 2 presents the vibrational frequencies of the 39 normal modes of 2PYH<sub>2</sub>O calculated at the MP2/cc-pVTZ level of theory. The vibrations in Table 2 are sorted with ascending frequency.

The numbering of the monomer modes follows the nomenclature of Varsanyi<sup>31</sup> for benzene analogues, completed for the intermolecular modes.<sup>32</sup> The respective vibration should be inspected as animated graphs with a viewer such as Molden or Molekel.<sup>33,34</sup> The Gaussian.log and Molcas.freq files, which contain the normal-mode analyses, can be downloaded from our home page.<sup>35</sup> The calculated frequencies are unscaled and compared to the experimental frequencies in Table 2.

**Experimental Results.** The bands labeled with an asterisk in the LIF spectrum of Figure 2 were excited to obtain the DF spectra that are shown in Figure 3. The assignment of these bands to specific vibrational modes in the excited state was made on the basis of the propensity rule from the intensities in the emission spectra and are given in the inset of Figure 2. The assignment will be explained below, together with a discussion of the respective ground-state vibrations.

Trace a of Figure 3 shows the fluorescence emission spectrum obtained via excitation of the vibrationless origin 0,0. The assignments given in Figure 3 are based on the ab initio calculations described earlier in this section. The calculated frequencies for the ground-state vibrations that were used for the assignment are summarized in Table 2.

The strongest band in the emission spectrum after excitation at 0,0 + 122 cm<sup>-1</sup> (trace c of Figure 3) is found at 137 cm<sup>-1</sup> and can be assigned on the basis of MP2 calculations to the intermolecular  $\beta_1$  vibration. The corresponding computed frequency is quite close (165 cm<sup>-1</sup>) (see Table 2). The  $\beta_1$  mode can be described as an in-plane wagging mode of the water moiety with respect to the 2PY moiety. Combination bands with the vibrations  $\sigma$ , 6a, 6b, 1, 9a, and  $\nu(\text{C}=\text{O})$  can be identified. The assignment of the 122 cm<sup>-1</sup> band in the absorption spectrum to  $\beta_1$  in the S<sub>1</sub> state therefore appears sound.

Although the following transition at 0,0 + 140 cm<sup>-1</sup> belongs to the pyridone–water spectrum as has been shown via the rotational constants by Held and Pratt,<sup>14</sup> no dispersed fluorescence spectrum could be detected after excitation of this band. Only the resonance fluorescence and stray light were observed. Held and Pratt<sup>14</sup> assigned this band on the basis of the large inertial defect in the excited state to an intermolecular out-of-plane vibration, possibly a torsional motion of the water moiety. Because the energetically following band at 155 cm<sup>-1</sup> again shows a sharp, resonant dispersed fluorescence spectrum, the reason for this disappearance cannot be a low-lying dissociation energy. One might conjecture that the dissociation is mode-specific along this selected coordinate.

Excitation at 155 cm<sup>-1</sup> (trace e of Figure 3) results in a long progression up to the third overtone of a band at 175 cm<sup>-1</sup> and combination bands with the modes  $\beta_1$ , 6a, 6b, 1, 9a, and

$\nu(\text{C}=\text{O})$ . The MP2 calculations allow a straightforward assignment of the S<sub>1</sub> vibration at 155 cm<sup>-1</sup> to mode  $\sigma$ , which can be described as a stretching vibration of the water moiety relative to the pyridone monomer.

**Geometry Fit Results.** The program *pKrFit* was used to estimate the structure of 2PYH<sub>2</sub>O in the S<sub>0</sub> and S<sub>1</sub> state from the rotational constants that have been determined by Held and Pratt.<sup>14</sup> We performed a fit of the structural parameters given in Table 3 to the rotational constants of eight different isotopomers. For a nonplanar molecule, this results in 24 inertial parameters that can be used for the fit. To have an overdetermined system of equations for the fit, a maximum of 23 geometry parameters can be used.

For the determination of the structure in the ground state, the results of the ab initio calculation at the MP2 level were taken as starting geometry. As fit parameters, we chose the lengths of all ring bonds, the CO bond length, the OO distance, the amino bond, and the OH bond included in the hydrogen bond. Furthermore, we fit three angles and five dihedral angles specified in Table 3 that describe the cluster geometry as well as the planarity of the 2PY moiety.

For the determination of the structure in the excited state, the results of our fit ground-state geometry were taken as starting geometry. We took the same fit parameters as for the ground state with one exception. The OH bond included in the hydrogen bond was fit to no physically reasonable value (lower than 90 pm). Thus, we kept this coordinate fixed at different values and subsequently performed fits of the remaining parameters. The best fit was obtained by keeping the value of the OH bond at 91 pm.

The fit results are presented in Table 3. The 2PY monomer moiety is slightly distorted out of plane in the excited state, although the values are afflicted with relatively high errors, cf. Table 3. The pyridone ring is distorted asymmetrically, with a mean increase of ring bond lengths of 0.2 pm, while the CO bond increases by 5.3 pm upon excitation. The hydrogen bond between the carbonyl group and the water moiety is extremely weakened and shows an increase of 20.4 pm. The weakening of the second hydrogen bond between the amino group of pyridone and water is less-pronounced, as reflected by an increase of bond length of only 4.3 pm. As a result of both hydrogen bonds being considerably destabilized upon excitation, the origin of the cluster is strongly blue-shifted (632.3 cm<sup>-1</sup>) with regard to the monomer. The maximum deviations of the fit rotational constants to the experimentally determined ones are 0.6 MHz for the ground state and 1.2 MHz for the excited states.

Subsequently, the geometry changes of 2PYH<sub>2</sub>O were fit to the line intensities in the emission spectra and to the changes of the rotational constants. Ninety three line intensities from three fluorescence emission spectra and the rotational constants changes of eight different isotopomers were used for the fit. Emission spectra have been obtained from excitation of 0,0,  $\beta_1$ , and  $\sigma$ . These modes were taken as displacement vectors for the fit. Additionally, the ring modes 15, 6a, 6b, 1, 9a, and the C=O stretch vibration were included in the fit because all modes show up in the DF spectra as fundamentals as well as combination bands with the intermolecular vibrations  $\beta_1$  and  $\sigma$ . Thus, we use eight motions as basis for the displacements upon electronic excitation. All of them are intermolecular or in-plane modes and are depicted in Figure 4.

The results of the combined fits of the intensities (93 data points) in the spectra of Figure 3 and the changes of the rotational constants of eight isotopomers (24 data points) by displacing the S<sub>1</sub>-state geometry along the eight normal modes

**TABLE 2:** MP2/cc-pVTZ Calculated Harmonic Ground-State Vibrational Frequencies and Description of the Motions of 2PYH<sub>2</sub>O<sup>a</sup>

assignment	calcd	obsd	obsd/calcd	assignment	calcd	obsd	obsd/calcd
$\rho_1$	69	62 <sup>b</sup>	0.90	18a	1041		
$\beta_1$	162	137	0.85	18b	1126		
10b	184			9b	1170		
$\sigma$	203	175	0.86	9a	1251	1247	1.00
$\rho_2$	264	189	0.72	8b	1310		
16a	397			3	1409		
$\tau$	432			19b	1478		
15	482	475	0.99	8a	1518		
16b	521			19a	1596		
6a	552	546	0.99	14	1660		
6b	619	611	0.99	$\delta$ HOH	1682		
4	732			$\nu$ C=O	1757	1702	0.97
CH (inv)	779			$\nu$ CH	3216		
$\beta_2$	813			$\nu$ CH	3244		
1	845	828	0.98	$\nu$ CH	3255		
CH (inv)	865			$\nu$ CH	3272		
NH + CH (inv)	910			$\nu$ NH <sub>bond</sub>	3361	3329 <sup>7</sup>	0.99
NH + CH (inv)	963			$\nu$ OH <sub>bond</sub>	3501	3346 <sup>7</sup>	0.96
CH (inv)	998			$\nu$ OH <sub>free</sub>	3916	3725 <sup>7</sup>	0.95
12	1003	968	0.97				

<sup>a</sup> All frequencies are given in cm<sup>-1</sup>. The numbering follows the nomenclature of Varsanyi<sup>31</sup> for benzene analogues, completed for the intermolecular modes.<sup>32</sup> <sup>b</sup> Obtained from the first overtone in harmonic approximation.

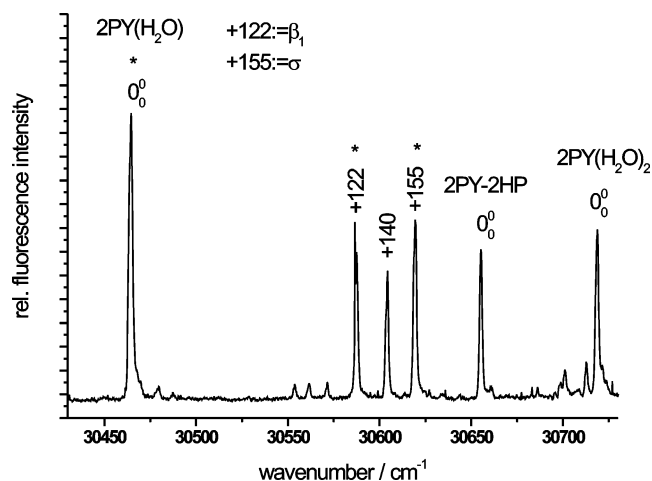


**Figure 2.** LIF spectrum of the 2-pyridone–water cluster. The bands labeled with an asterisk were excited to obtain the DF spectra that are shown in Figure 3.

described above are shown in Figure 3. Close inspection of all emission spectra shows that the intensity pattern is well-reproduced upon displacement of the S<sub>1</sub> geometry. Taking the S<sub>0</sub> and S<sub>1</sub> geometries resulted in an FC pattern completely different from the observed ones.

Table 4 summarizes the results for the S<sub>1</sub> displacements. The 2PY moiety remains planar upon electronic excitation, and the ring expands unsymmetrically. The hydrogen bond O7H7 is elongated strongly, whereas the other hydrogen bond is shortened slightly. The first column presents the results for the geometry changes upon electronic excitation as obtained from the CASSCF calculations. The second column shows the results for the geometry changes from the fit to the rotational constants. The third column shows the results for the geometry changes from the Franck–Condon fit and to the changes of the rotational constants. The fourth column gives the experimentally determined rotational constant changes and estimated intermolecular distances by Held and Pratt.<sup>14</sup> Figure 5 shows the geometry changes upon electronic excitation from the combined FC/rotational constants fit in graphical form.

The results of the above-mentioned fits to the structural changes obtained from ab initio calculations (CASSCF) are

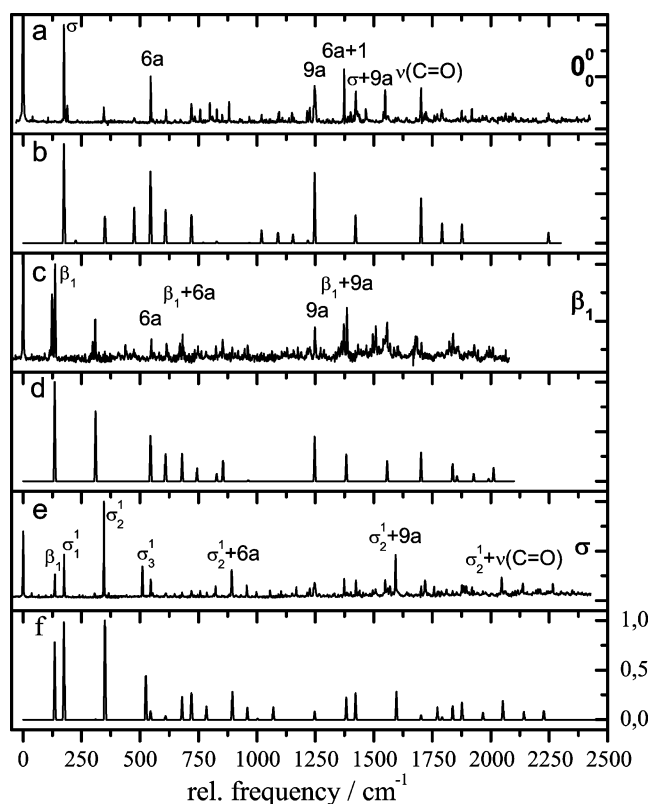


**Figure 3.** Comparison of experimental and simulated fluorescence emission spectra of the 2-pyridone–water cluster. Trace a shows the experimental DF spectrum, obtained by excitation of the electronic origin. Trace b gives the results of the FC fit, described in the text. The experimental DF spectrum obtained via excitation of 0,0 + 122 cm<sup>-1</sup> is depicted in trace c, the respective fit in trace d. Traces e and f show the experimental and fit DF spectra via excitation of 0,0 + 155 cm<sup>-1</sup>. The simulated intensities are plotted using experimental wavenumbers to facilitate the comparison of the intensities.

compared in Table 4. The experimentally determined changes of the rotational constants are very well-matched by both fits in contrast to the results of the CASSCF calculations. The ab initio calculations, as well as the structure fit using the rotational constants, show a strong distortion of the pyridone moiety but

TABLE 3: Results of the  $r_0$  Structure Fit for 2PYH<sub>2</sub>O<sup>a</sup>

	$S_0(r_0)$	$S_1(r_0)$	fitted parameters	$S_0(r_0)$	$S_1(r_0)$
[NHHOH] <sup>b</sup>			bond length/pm		
A/MHz	3996.9(-0.4)	3934.6(-1.2)	N1–C2	141.4(3)	144.7(2)
B/MHz	1394.2(-0.1)	1348.2(±0.0)	C2–C3	144.3(4)	145.3(6)
C/MHz	1034.8(±0.0)	1006.4(±0.0)	C3–C4	135.9(9)	139.7(16)
$\Delta I^c$	-0.55(0.03)	-0.59(±0.0)	C4–C5	142.8(3)	125.7(12)
[NHH <sup>18</sup> OH] <sup>b</sup>			N1–C6	134.0(8)	124.5(7)
A/MHz	3970.7(±0.0)	3911.0(0.2)	C2–O7	125.6(3)	130.9(9)
B/MHz	1325.5(-0.1)	1280.4(0.1)	O7–O8	270.3(5)	288.4(5)
C/MHz	994.8(±0.0)	966.7(-0.1)	N1–H1	100.2(8)	96.1(10)
$\Delta I^c$	-0.53(0.03)	-0.61(-0.02)	O8–H7	93.9(17)	91.0 <sup>d</sup>
[NDHOH] <sup>b</sup>			angle/deg		
A/MHz	3958.6(-0.2)	3902.4(-0.7)	C2–O7–O8	100.4(2)	97.3(3)
B/MHz	1389.2(±0.0)	1343.2(0.1)	H7–O8–O7	19.9(4)	20.0(2)
C/MHz	1029.5(-0.1)	1001.5(±0.0)	H8–O8–O7	120.2(15)	118.7(10)
$\Delta I^c$	-0.56(-0.04)	-0.57(0.04)	dihedral angle/deg		
[NHDOH] <sup>b</sup>			C2–C3–C4–C5	0(34)	-11(12)
A/MHz	3995.6(0.1)	3933.5(0.7)	N1–C2–C3–C4	0(8)	5(8)
B/MHz	1366.0(-0.1)	1320.2(-0.3)	C6–N1–C2–C3	0(16)	6.5(4)
C/MHz	1019.1(0.1)	990.6(±0.0)	O8–O7–C2–C3	178(9)	183(7)
$\Delta I^c$	-0.55(0.07)	-0.56(±0.0)	H8–O8–O7–C2	140(7)	135.9(5)
[NHHOD] <sup>b</sup>					
A/MHz	3978.5(0.6)	3914.3(0.3)			
B/MHz	1337.7(0.3)	1294.3(0.3)			
C/MHz	1003.0(-0.1)	975.9(-0.2)			
$\Delta I^c$	-0.96(-0.16)	-0.76(-0.06)			
[NDDOH] <sup>b</sup>					
A/MHz	3957.1(0.4)	3901.1(0.9)			
B/MHz	1361.4(±0.0)	1315.6(-0.1)			
C/MHz	1014.0(0.2)	986.0(0.2)			
$\Delta I^c$	-0.53(0.09)	-0.60(0.02)			
[NHDOD] <sup>b</sup>					
A/MHz	3976.8(-0.3)	3912.8(±0.0)			
B/MHz	1312.3(0.1)	1269.1(±0.0)			
C/MHz	988.6(-0.1)	961.4(-0.1)			
$\Delta I^c$	-0.98(-0.07)	-0.72(0.02)			
[NDDOD] <sup>b</sup>					
A/MHz	3939.6(-0.2)	3881.6(-0.3)			
B/MHz	1308.3(-0.1)	1265.0(±0.0)			
C/MHz	984.0(-0.1)	957.3(-0.1)			
$\Delta I^c$	-0.97(-0.01)	-0.81(-0.02)			

<sup>a</sup> The deviations of the experimentally determined rotational constants and inertial defects are given in brackets after the respective rotational constant as  $\Delta R = R_{\text{calcd}} - R_{\text{expt}}$  and  $\Delta I = I_{\text{calcd}} - I_{\text{expt}}$ . <sup>b</sup> [NHHOH] refers to atoms N1H1H7O8H8, cf. Figure 1. <sup>c</sup> In the  $S_1$  column the value of  $\Delta I = \Delta I_{S_1} - \Delta I_{S_0}$  is given with the deviations in parentheses. <sup>d</sup> Bond length kept fixed on this value.

with no overall expansion of the ring (6-ring (mean): +0.1 and +0.2 pm, respectively). The Franck–Condon fit shows an unsymmetrical distortion and a slight overall expansion of the ring (6-ring (mean): +1.2 pm). The hydrogen bond strength of O7H7 decreases upon electronic excitation for all methods. The decrease is slightly larger than that calculated by Held and Pratt. The difference can be traced back to the different models used. While in ref 14 it was assumed that both monomer moieties remain unchanged upon complexation, we also fit monomer structural parameters. A check of whether the used model is good can be performed by calculating the atom positions in our fit  $S_0$  and  $S_1$  structures. They should agree within the experimental accuracy with the center-of-mass coordinates determined by Held and Pratt. Table 5 compares these coordinates. They agree very well with the exception of the  $|y|$  coordinate of the “free” hydrogen atom of the water moiety.

The hydrogen bond length O8H1 decreases for the CASSCF calculations and the Franck–Condon fit with the former one being 3 times larger than the latter one. The structure fit to the rotational constants shows an increased bond length similar to that evaluated by Held and Pratt.

In contrast to the geometry of the monomer, which has been shown to be planar in the electronic ground state but nonplanar in the electronically excited state, a nearly planar monomer

geometry in the cluster is found for both electronic states.<sup>14</sup> This can be seen by comparing the changes of the inertial defects of the cluster upon electronic excitation (given in Table 3) with the ones of the pyridone monomer from ref 14. Although the changes  $\Delta I$  are between -0.5 and -0.6 amu Å<sup>2</sup> for the cluster, they range from -1.3 to -1.5 amu Å<sup>2</sup> for the monomer. Thus, in spite of vibrationally averaged out-of-plane position of the exocyclic (free) hydrogen atom of the water moiety, the changes of the inertial defect upon electronic excitation are considerably smaller for the cluster than for the monomer. Held and Pratt made ionic resonance structures with partial C=N double bond character in the amide group responsible for this finding.

This effect is fully confirmed by the ab initio calculations. Figure 6 shows Wiberg bond indices and partial charges from a NBO analysis using the results of the CASSCF wavefunctions. Going from a to b in Figure 6 represents electronic excitation of the monomer, a to c cluster formation in the electronic ground state, and c to d electronic excitation of the cluster. Complexation (a to c) leads to an increase of negative charge on the oxygen atom O7 and an increase of positive charge on the nitrogen atom N1, accompanied by a very small increase in bond order between N1 and C2, pointing to a partial  $\text{O}^-\text{C}=\text{N}^+-\text{H}$  character of the *cis*-amide bond in pyridone. This “quasi-ionic” structure is stabilized by dipole–dipole interactions with

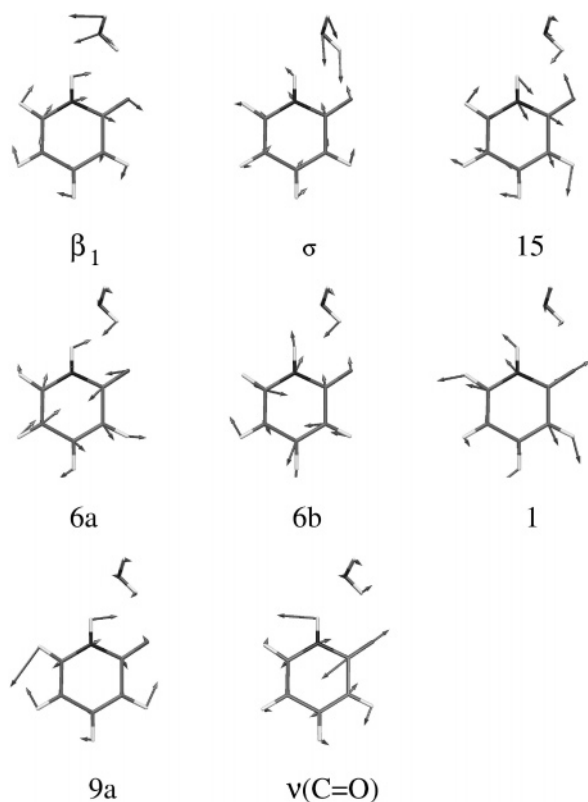


**Figure 4.** Normal modes that are used as a basis for the structure fit in the electronically excited state.

**TABLE 4: Comparison of the Geometry Changes of 2PYH<sub>2</sub>O upon Electronic Excitation from a CASSCF(8,7) Study, from the Structural Fit to the Rotational Constants, and from the Franck–Condon Fit Described in the Text<sup>a</sup>**

$S_1-S_0$	CASSCF	pKrFit	FC fit	expt <sup>14</sup>
N1–C2	–0.7	+3.3	+2.2	
C2–C3	–10.2	+1.0	–2.4	
C3–C4	+12.1	+3.8	+9.2	
C4–C5	–8.1	–17.1	–6.8	
C5–C6	+8.5	+19.9	+10.3	
C6–N1	–1.2	–9.5	–5.1	
6-ring (mean)	+0.1	+0.2	+1.2	
C2–O7	+11.5	+5.3	+4.2	
N1–H1	+0.1	–4.1	±0.0	
O8–H7	–0.4	–2.9	–2.0	
O7–H7	+29.4	+20.4	+25.7	+8.0
O8–H1	–7.7	+4.3	–2.4	+10.0
N1–O8	–0.4	+4.3	+5.1	+11.0
O7–O8	+12.7	+18.1	+8.5	+14.0
$\Delta A/\text{MHz}$	–125.0	–62.3	–62.0	–63.1
$\Delta B/\text{MHz}$	–27.0	–46.0	–43.3	–45.9
$\Delta C/\text{MHz}$	–23.0	–28.4	–28.4	–28.4

<sup>a</sup> All bond length changes are given in pm.

the water molecule. Electronic excitation in the monomer shifts electron density from O7 into the ring, thus reducing the negative charge at O7 and increasing the C2C3 and C4C5 bond order, while the C3C4 bond order decreases. Therefore, quasi-ionic structures as in the ground state play a much smaller role in the excited state, and the water cluster is accordingly destabilized upon excitation. The hydrogen bond order index O7H7 decreases nearly by a factor of 10, while the two water OH bonds get more similar in the excited state.

#### 4. Conclusions

We report the determination of the structural changes of the 2PY–water cluster upon electronic excitation from a combined

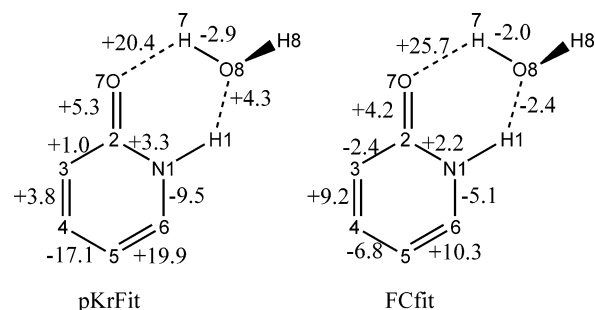


**Figure 5.** Schematic drawing of the geometric changes in the 2-pyridone–water cluster upon electronic excitation.

**TABLE 5: Comparison of Selected Center-of-Mass Coordinates of Atoms in the Pyridone–Water Cluster Calculated from the Fit Structures of This Publication and from a Kraichman Analysis Given in Ref 14<sup>a</sup>**

	$S_0$ coordinates						
	x		y		z		
	here	ref <sup>14</sup>	here	ref <sup>14</sup>	here	ref <sup>14</sup>	
H1	114	114	111	112	2	20	
H7	274	274	20	17	4	30	
H8	389	389	63	71	50	40	
O8	308	309	67	68	4	0	
	$S_1$ coordinates						
	H1	117	117	103	103	10	20
	H7	283	283	20	–	2	30
	H8	391	392	61	74	57	50
O8	317	317	65	65	4	0	

<sup>a</sup> Atomic numbering refers to Figure 5.

fit of the line intensities in the fluorescence emission spectra and the changes of the rotational constants upon electronic excitation, as well as from a fit to the absolute rotational constants in each electronic state. Each of the fits is performed with different sets of coordinates, whose choice is governed by the applied method. The fit to the absolute rotational constants is performed in a set of  $3N - 6$  internal coordinates. For a complete structure determination, this requires at least the same number of inertial parameters if no symmetry is present. For larger molecules, such a vast number of isotopic data is generally not available, and selected coordinates have to be kept fixed to physically reasonable values in the fit or to values, which are known from other, but similar molecules. Such model restrictions, of course, limit the applicability of the fit. The fit to the line intensities and to the changes of the rotational constants uses a completely different set of coordinates. Because the natural choice for a basis of displacement coordinates in the computation of Franck–Condon integrals are the normal modes of the molecule in one of the electronic states, we use a linear combination of normal-mode displacement vectors in the geometry fit. Nevertheless, this method has the same drawback as the fit in internal coordinates: only normal modes, which have been assigned unambiguously to observed transitions in the emission spectrum, form the basis for the distortion of the molecule. Thus, the number of geometry parameters to be fit exceeds the number of experimental data points. Because both coordinate sets are very different, and completely independent, a comparison of the geometry changes obtained by both methods helps to judge the reliability and completeness of the basis for the geometry changes.

In the case of the 2PY–water cluster, we were able to show that the pyridone moiety remains planar upon electronic excitation in contrast to the 2PY monomer. Using an NBO analysis, we could show that quasi-ionic structures, which are

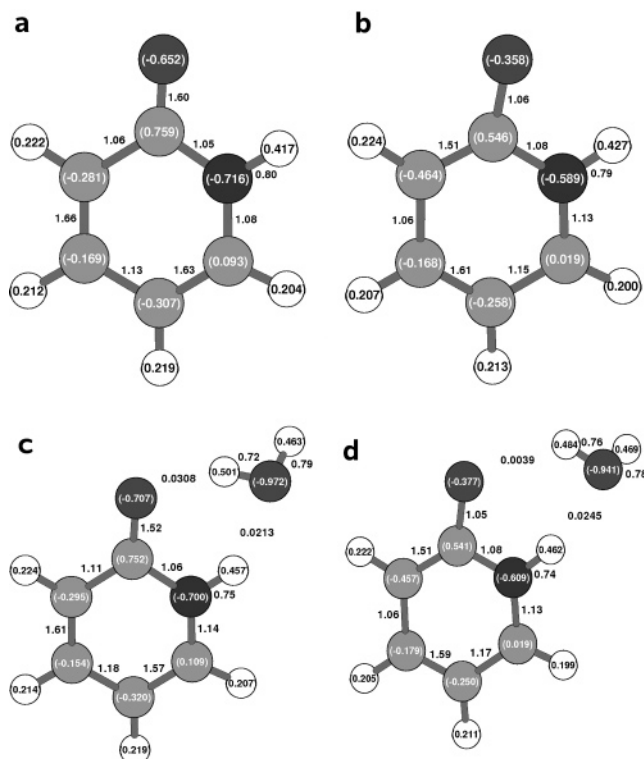


**Figure 6.** Charges and Wiberg bond indices calculated via natural bond orbital analysis. Calculations were performed using the CASSCF-(8,7) wavefunction with Dunning's correlation consistent double- $\zeta$  basis set cc-pVDZ. Depicted are (a) 2PY in the ground state, (b) 2PY in the first excited singlet state, (c) 2PYH<sub>2</sub>O in the ground state, and (d) 2PYH<sub>2</sub>O in the first excited singlet state.

made responsible for this effect, contribute considerably to the resonance structures of 2PY–water. The geometry parameters could be determined more accurately than with a fit to the inertial parameters or the intensities alone, resulting in a higher reliability of the so-obtained structures.

**Acknowledgment.** The financial support of the Deutsche Forschungsgemeinschaft (KL531/22) is gratefully acknowledged. We thank Dr. D. Krügler for helpful discussions. We thank the Universitätsrechenzentrum Köln for the granted computing time.

## References and Notes

- Held, A.; Champagne, B.; Pratt, D. *J. Chem. Phys.* **1991**, *95*, 8732–8743.
- Hatherley, L.; Brown, R.; Godfrey, P.; Pierlot, A.; Caminati, W.; Damiani, D.; Melandri, S.; Favero, L. *J. Phys. Chem.* **1993**, *97*, 46–51.
- Tanjaroon, C.; Subramanian, R.; Karunatilaka, C.; Kukolich, S. *J. Phys. Chem. A* **2004**, *108*, 9531–9539.
- Piacenza, M.; Grimme, S. *J. Comput. Chem.* **2003**, *25*, 83–98.
- Florio, G.; Gruenloh, C.; Quimpo, R.; Zwier, T. *J. Chem. Phys.* **2000**, *113*, 11143–11153.

- Maris, A.; Ottaviani, P.; Caminati, W. *Chem. Phys. Lett.* **2002**, *360*, 155–160.
- Matsuda, Y.; Ebata, T.; Mikami, N. *J. Chem. Phys.* **1999**, *110*, 8397–8407.
- Matsuda, Y.; Ebata, T.; Mikami, N. *J. Chem. Phys.* **2000**, *113*, 573–580.
- Dkhissi, A.; Adamowicz, L.; Maes, G. *Chem. Phys. Lett.* **1991**, *324*, 127–136.
- Topal, M. D.; Fresco, J. R. *Nature* **1976**, *263*, 285–289.
- Griffiths, A. J. F.; Gelbart, W. M.; Miller, J. H.; Lewontin, R. C. *Modern Genetic Analysis*; W. H. Freeman and Company: New York, 1999.
- Nowak, M.; Lapinski, L.; Fulara, J.; Les, A.; Adamowicz, L. *J. Phys. Chem.* **1992**, *96*, 1562–1569.
- Nimlos, M.; Kelley, D.; Bernstein, E. *J. Phys. Chem.* **1989**, *93*, 643–651.
- Held, A.; Pratt, D. *J. Am. Chem. Soc.* **1993**, *115*, 9708–9717.
- Held, A.; Pratt, D. W. *J. Chem. Phys.* **1992**, *96*, 4869–4876.
- Held, A.; Pratt, D. W. *J. Am. Chem. Soc.* **1990**, *112*, 8629–8630.
- Borst, D. R.; Roscioli, J.; Pratt, D.; Florio, G.; Zwier, T.; Müller, A.; Leutwyler, S. *Chem. Phys. Lett.* **2002**, *341*, 341–354.
- Frey, J. A.; Leist, R.; Tanner, C.; Frey, H.-M.; Leutwyler, S. *J. Chem. Phys.* **2006**, *125*, 114308.
- Barone, V.; Adamo, C. *Int. J. Quantum Chem.* **1997**, *61*, 429–441.
- Li, Q.; Fang, W.; Yu, J. *J. Phys. Chem. A* **2005**, *109*, 3983–3990.
- Kraitchman, J. *Am. J. Phys.* **1953**, *21*, 17.
- Costain, C. *J. Chem. Phys.* **1958**, *29*, 864.
- Ratzer, C.; Küpper, J.; Spangenberg, D.; Schmitt, M. *Chem. Phys.* **2002**, *283*, 153–169.
- Schmitt, M.; Krügler, D.; Böhm, M.; Ratzer, C.; Bednarska, V.; Kalkman, I.; Meerts, W. L. *Phys. Chem. Chem. Phys.* **2006**, *8*, 228–235.
- Schmitt, M.; Henrichs, U.; Müller, H.; Kleinermanns, K. *J. Chem. Phys.* **1995**, *103*, 9918–9928.
- Roth, W.; Jacoby, C.; Westphal, A.; Schmitt, M. *J. Phys. Chem. A* **1998**, *102*, 3048–3059.
- Frisch, M. J.; Trucks, G. W.; Schlegel, H. B.; Scuseria, G. E.; Robb, M. A.; Cheeseman, J. R.; Montgomery, J. A., Jr.; Vreven, T.; Kudin, K. N.; Burant, J. C.; Millam, J. M.; Iyengar, S. S.; Tomasi, J.; Barone, V.; Mennucci, B.; Cossi, M.; Scalmani, G.; Rega, N.; Petersson, G. A.; Nakatsuji, H.; Hada, M.; Ehara, M.; Toyota, K.; Fukuda, R.; Hasegawa, J.; Ishida, M.; Nakajima, T.; Honda, Y.; Kitao, O.; Nakai, H.; Klene, M.; Li, X.; Knox, J. E.; Hratchian, H. P.; Cross, J. B.; Bakken, V.; Adamo, C.; Jaramillo, J.; Gomperts, R.; Stratmann, R. E.; Yazyev, O.; Austin, A. J.; Cammi, R.; Pomelli, C.; Ochterski, J. W.; Ayala, P. Y.; Morokuma, K.; Voth, G. A.; Salvador, P.; Dannenberg, J. J.; Zakrzewski, V. G.; Dapprich, S.; Daniels, A. D.; Strain, M. C.; Farkas, O.; Malick, D. K.; Rabuck, A. D.; Raghavachari, K.; Foresman, J. B.; Ortiz, J. V.; Cui, Q.; Baboul, A. G.; Clifford, S.; Cioslowski, J.; Stefanov, B. B.; Liu, G.; Liashenko, A.; Piskorz, P.; Komaromi, I.; Martin, R. L.; Fox, D. J.; Keith, T.; Al-Laham, M. A.; Peng, C. Y.; Nanayakkara, A.; Challacombe, M.; Gill, P. M. W.; Johnson, B.; Chen, W.; Wong, M. W.; Gonzalez, C.; Pople, J. A. *Gaussian 03*, revision B.04; Gaussian, Inc.: Wallingford, CT, 2004.
- Dunning, T. H., Jr. *J. Chem. Phys.* **1989**, *90*, 1007–1023.
- Karlström, G.; Lindh, R.; Malmqvist, P.-Å.; Roos, B. O.; Ryde, U.; Veryazov, V.; Widmark, P.-O.; Cossi, M.; Schimmelpfennig, B.; Neogrady, P.; Seijo, L. *Comput. Mater. Sci.* **2003**, *28*, 222–239.
- Spangenberg, D.; Imhof, P.; Kleinermanns, K. *Phys. Chem. Chem. Phys.* **2003**, *5*, 2505–2514.
- Varsanyi, G. *Assignments for Vibrational Spectra of 700 Benzene Derivatives*; Wiley: New York, 1974.
- Schütz, M.; Bürgi, T.; Leutwyler, S. *J. Chem. Phys.* **1992**, *99*, 3763–3776.
- Schafteenaar, G.; Noordik, J. H. *J. Comput.-Aided Mol. Des.* **2000**, *14*, 123–134.
- Molekel. Portmann, S. <http://www.cscs.ch/molekel/>, 2002.
- <http://www-public.rz.uni-duesseldorf.de/~pcl>, 2006.